

Analog Speed-Control of DC-Motor Using Proportional and Proportional-Integral Controllers

Deia Halboot Mohussen
Assist Lecturer
Al-Mustansiriya University
Engineering College
Computer and Software Dep.
deia_mohussen@yahoo.com

Abstract

A systematic development of the analysis, design, and testing by simulation of a closed-loop speed control of separately excited dc motor drive system is described in this paper. The motor controlled armature voltage is supplied from a three-phase fully controlled bridge converter. Closed-loop control is analyzed by using transfer function techniques and the necessity of an inner current control loop is demonstrated.

Designs of both a proportional and proportional-integral controllers are outlined by using transfer function technique. A soft starting concept is used to reduce the value of starting current. The feed forward loop is used to reduce the effect of load torque disturbances. The speed and current responses are also presented for load and no-load cases.

الخلاصة

تحليل وتصميم واختبار بالمحاكاة لنظام الحلقة المغلقة للسيطرة على سرعة نظام سواقه محرك تيار مستمر ذو أثاره منفصلة تم وصفها في هذا البحث. فولتية الحرض المسيطر عليها تم تجهيزها عبر محول قدرة متناوبة الى قدرة مستمرة ثلاثي الطور جسري.

نظام السيطرة بالحلقة المغلقة تم تحليله باستخدام تقنية دالة التحويل وتم بيان الحاجة الى حلقة تيار داخلية. تصميم كل من المسيطر-P والمسيطر-PI بين باستخدام تقنية دالة التحويل. لتقليل تيار بدء التشغيل تم استخدام مفهوم بدء التشغيل الناعم أو المتدرج. حلقة التغذية الأمامية تم استخدامها لتقليل تأثير الاضطرابات التي تحدث بسبب الحمل. استجابة التيار والسرعة للنظام تم تثبيتها لحالتي الحمل وبدون حمل.

1. Introduction

DC drives, being easy to control, are widely used in many variable-speed drive systems [1]. Open-loop operation of dc motors may not be satisfactory in many applications. However, if the drive requires constant speed operation the firing angle has to change to maintain a constant speed. This can be achieved in a closed-loop control system. A closed-loop system generally has the advantages of greater accuracy, improved dynamic response, and reduced effects of disturbances such as loading. When the drive requirements include rapid acceleration and deceleration, closed-loop control is necessary. In a closed-loop system even the drive characteristics can be modified. Thus, the system can be made to operate at constant torque or constant horsepower over a certain speed range. Circuit protection (current limiter) can be provided in a closed-loop system [2]. In this paper the response of closed-loop system and control design studied by using transfer function techniques. The necessity and significance of the control loops and different parameters are shown. For simplicity and ease of understanding, the system is reduced to the lowest possible order by neglecting some smaller time constants.

2. Closed-Loop Control system

The basic block diagram of close-loop control system is shown in Fig. 1. The error $\epsilon_w(s)$ used to control the armature voltage. The applied armature voltage is controlled using a three-phase fully controlled bridge converter. If the appropriate firing control technique employed a linear relationship between the control voltage E_c and the armature voltage E_a can be obtained, therefore the converter behave essentially as a power amplifier with a linear voltage transfer characteristic [3-5]. If the small delay time associated with the converter is neglected, then

$$\frac{E_a(s)}{E_c(s)} = K_c = \frac{3\sqrt{6} V_{ph}}{\pi \hat{E}_c} \tag{1}$$

\hat{E}_c Corresponds to 0° firing angle and V_{ph} is the ac phase rms voltage.

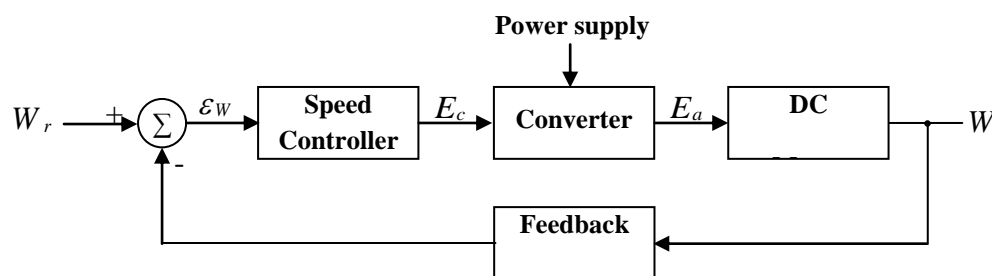


Fig. 1: Basic block diagram of a closed-loop speed-control system

2.1. DC-Motor Transfer Function

The speed control of the separately excited dc motor is relatively easy, because the separate excitation. Consider a separately excited dc motor with armature voltage control, as shown in Fig. 2a. The voltage loop equation is

$$e_a = e_g + R_a i_a + L_a \frac{di_a}{dt} \tag{2}$$

Where

$$e_g = k_a \phi \cdot w \tag{3}$$

The torque balance equation is

$$T = T_L + Bw + j \frac{dw}{dt} \tag{4}$$

Where

$$T = k_a \phi \cdot i_a \tag{5}$$

In the Laplace domain, equations (2) through (5) can be written as

$$E_a(s) = E_g(s) + R_a I_a(s) + sL_a I_a(s) \tag{6}$$

$$E_g(s) = k_a \phi \cdot W(s) \tag{7}$$

$$T(s) = T_L(s) + BW(s) + sJW(s) \tag{8}$$

$$T(s) = k_a \phi \cdot I_a(s) \tag{9}$$

Thus, from equation (6)

$$I_a(s) = \frac{E_a(s) - E_g(s)}{R_a + sL_a} = \frac{(E_a(s) - E_g(s)) / R_a}{1 + s\tau_a} \tag{10}$$

Where $\tau_a = L_a / R_a$ =electrical time constant of the motor armature circuit.

From equation (8)

$$W(s) = \frac{T(s) - T_L(s)}{B + sJ} = \frac{(T(s) - T_L(s)) / B}{1 + s\tau_m} \tag{11}$$

Where $\tau_m = J / B$ =mechanical time constant of the motor. These relationships are shown in block diagram form in Fig. 2b.

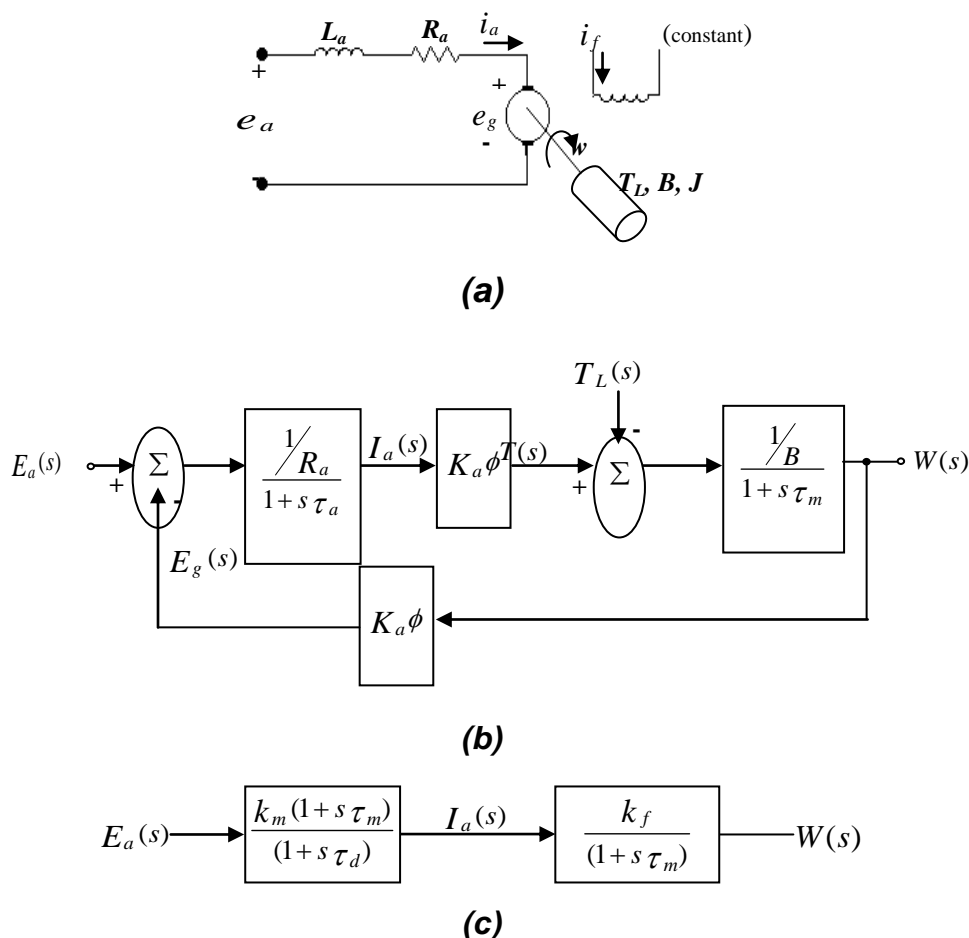


Fig. 2: Development of motor transfer function. (a) Separately excited dc motor model. (b) Functional block diagram (c) Simplified functional block diagram

Note the feedback loop present in the form of the back EMF. This provides the moderate speed regulation inherent in the separately excited dc motor [1, 6]. From Fig. 2b the change in speed $W(s)$ due to disturbances in applied voltage $E_a(s)$ and load torque $T_L(s)$ can be expressed in the following expression.

$$W(s) = \frac{k_a \phi}{(k_a \phi)^2 + R_a B(1+s\tau_a)(1+s\tau_m)} E_a(s) + \frac{R_a(1+s\tau_a)}{(k_a \phi)^2 + R_a B(1+s\tau_a)(1+s\tau_m)} T_L(s) \quad (12)$$

If we neglect the load torque term, from equation (12)

$$\frac{W(s)}{E_a(s)} = \frac{k_a \phi}{(k_a \phi)^2 + R_a B(1+s\tau_a)(1+s\tau_m)} \quad (13)$$

If $\tau_a \ll \tau_m$ (which is almost always the case), then τ_a can be neglected, and the expression simplifies to

$$\frac{W(s)}{E_a(s)} = \frac{k_a \phi}{(k_a \phi)^2 + R_a B + s R_a B \tau_m} = \frac{k_d}{1+s\tau_d} \quad (13a)$$

Where

$$\tau_d = \frac{R_a B}{(k_a \phi)^2 + R_a B} \tau_m \quad (13b)$$

$$k_d = \frac{k_a \phi}{(k_a \phi)^2 + R_a B} \quad (13c)$$

$$\tau_d \ll \tau_m$$

From Fig. 2b

$$\frac{W(s)}{I_a(s)} = \frac{k_a \phi / B}{1 + s \tau_m} = \frac{k_f}{1 + s \tau_m} \quad (14)$$

Therefore, from equations (13a) and (14)

$$\begin{aligned} \frac{I_a(s)}{E_a(s)} &= \frac{W(s)}{E_a(s)} \times \frac{I_a(s)}{W(s)} \\ &= \frac{k_d B(1 + s \tau_m)}{k_a \phi(1 + s \tau_d)} = \frac{k_m(1 + s \tau_m)}{(1 + s \tau_d)} \end{aligned} \quad (15)$$

Thus the motor can be represented, for the purpose of analyzing it for armature voltage control, as two blocks as shown in Fig. 2c. The gain constants k_m , k_f and k_d shown in Fig. 2c are as follows.

$$k_m = \frac{B}{(k_a \phi)^2 + R_a B} \quad (15a)$$

$$k_f = \frac{k_a \phi}{B} \quad (15b)$$

$$k_d = k_m k_f \quad (15c)$$

2.2. Closed-Loop Speed Control

Several types of speed controllers are possible, two of the more common ones are proportional (P) and proportional-integral (PI) [7]. First a proportional controller is used. From Fig. 3, the total transfer function is

$$\frac{W(s)}{W_r(s)} = \frac{k_s k_c k_m k_f}{(1 + s \tau_d) + k_s k_c k_m k_f k_t} = \frac{k_1}{1 + s \tau_1} \quad (16)$$

Where k_s is proportional controller constant.

let

$$k_1 = \frac{k_s k_c k_m k_f}{k_s k_c k_m k_f k_t + 1}$$

and

$$\tau_1 = \frac{\tau_d}{k_s k_c k_m k_f k_t + 1}$$

If $k_s k_c k_m k_f k_t \gg 1$, then $k_1 \approx \frac{1}{k_t}$ and $\tau_1 = \frac{\tau_d}{k_s k_c k_m k_f k_t}$

Also

$$\frac{I_a(s)}{W_r(s)} = \frac{W(s)}{W_r(s)} \times \frac{I_a(s)}{W(s)} = \frac{k_1(1+s\tau_m)}{k_f(1+s\tau_1)} \tag{17}$$

The current response to a step change in input W_r is

$$I_a(s) = \frac{k_1 W_r (1+s\tau_m)}{k_f s(1+s\tau_1)} = \frac{A_1}{s} + \frac{A_2}{s + 1/\tau_1}$$

Where

$$A_1 = \frac{k_1 W_r}{k_f}$$

$$A_2 = \frac{k_1 W_r}{k_f \tau_1} (\tau_m - \tau_1)$$

$$I_a(t) = \frac{k_1 W_r}{k_f} \left[1 + \frac{(\tau_m - \tau_1) e^{-t/\tau_1}}{\tau_1} \right] \tag{18}$$

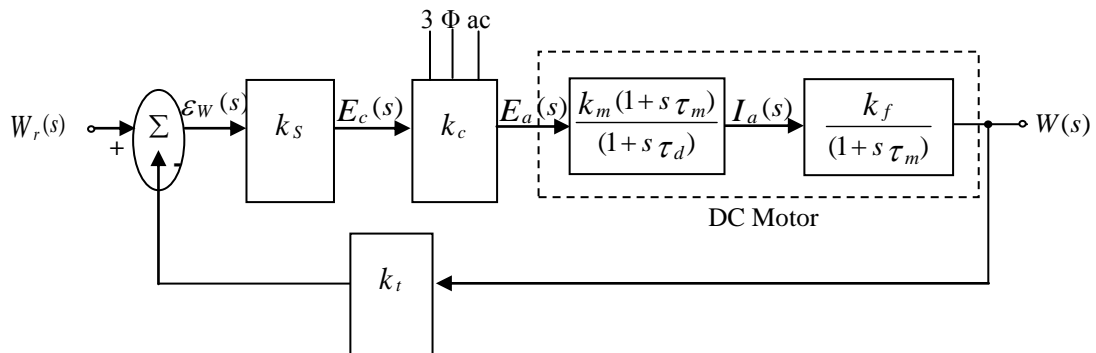


Fig. 3: Speed-control loop

The transient over current is undesirable from the standpoint of converter rating and protection. An input changes in W_r results a transient over current, this sudden change in current which decays slowly according to equation (18). The previous analysis reveals that it would be better to limit the current to maximum allowable value. This limiting can not be using the configuration of Fig. 3 where the motor voltage is controlled by the speed error. Any attempt to clamp this speed error will limit the motor voltage.

If armature losses are neglected, clamping the speed error will limit the speed, but not the current. However, a current limit can be implemented if we first construct an inner current-control loop using the clamped speed error as the current reference [2, 6].

2.3. Closed-Loop Current Control

The inner current control loop is shown in Fig. 4. In this figure the gain of the current controller is k_I , which here is assumed to be a proportional controller. A current feedback signal can be getting via a current transducer (sampling resistor) in the armature circuit. The gain of the current transducer is k_r . From Fig. 4 the transfer function is

$$\frac{I_a(s)}{I_r(s)} = \frac{k_I k_c k_m \frac{(1+s\tau_m)}{(1+s\tau_d)}}{1+k_r k_I k_c k_m \frac{(1+s\tau_m)}{(1+s\tau_d)}} = k_{IC} \frac{(1+s\tau_m)}{(1+s\tau_{m2})} \tag{19}$$

Where

$$k_{IC} = \frac{k_I k_c k_m}{1+k_r k_I k_c k_m} \tag{19a}$$

$$\tau_{m2} = \frac{\tau_m k_r k_I k_c k_m + \tau_d}{1+k_r k_I k_c k_m} \tag{19b}$$

Since $k_r k_I k_c k_m \gg 1$

$$k_{IC} \approx \frac{1}{k_r} \tag{20}$$

and

$$\tau_{m2} = \tau_m + \frac{\tau_d}{k_r k_I k_c k_m} \tag{20a}$$

Also $\tau_m \gg \tau_{m1}$, therefore

$$\tau_{m2} \approx \tau_m \tag{20b}$$

From equations (19) and (20b), it appears that a pole-zero cancellation is possible, resulting in no overshoot or time delay. Then;

$$\frac{I_a(s)}{I_r(s)} = k_{IC} \approx \frac{1}{k_r} \tag{21}$$

Because I_a is directly related to I_r , a limit on I_r will effectively limit the current. This inner loop can now be incorporated within the speed-control loop, using the clamped speed error as the current reference I_r . The implementation of this scheme is shown in the block diagram of Fig. 5a. The block diagram can be simplified, by using expression (21) and by neglecting the nonlinear clamping, to the diagram in Fig. 5b. Referring to Fig. 5b,

$$\frac{W(s)}{W_r(s)} = \frac{k_s k_{IC} k_f \frac{1}{(1+s\tau_m)}}{1 + \frac{k_s k_{IC} k_f k_t}{(1+s\tau_m)}} = \frac{k_2}{1+s\tau_2} \quad (22)$$

Where

$$k_2 = \frac{k_s k_{IC} k_f}{k_s k_{IC} k_f k_t + 1} \quad (22a)$$

$$\tau_2 = \frac{\tau_m}{k_s k_{IC} k_f k_t + 1} \quad (22b)$$

For $k_s k_{IC} k_f k_t \gg 1$,

$$k_2 \approx \frac{1}{k_t} = k_1 \quad (22c)$$

and

$$\tau_2 \approx \frac{\tau_m}{k_s k_{IC} k_f k_t}$$

Also, from equations (22) and (14)

$$\frac{I_a(s)}{W_r(s)} = \frac{W(s)}{W_r(s)} \times \frac{I_a(s)}{W(s)} = \frac{k_2(1+s\tau_m)}{k_f(1+s\tau_2)} \quad (23)$$

While equation (23) is not very different from equation (17), the expression in the former equation is only true while I_a is less than the limiting value. If, during acceleration or load changes, the speed error is large such that I_r is clamped at the maximum value \hat{I}_r , the current is limited to a maximum value $\hat{I}_a = k_{IC} \hat{I}_r$.

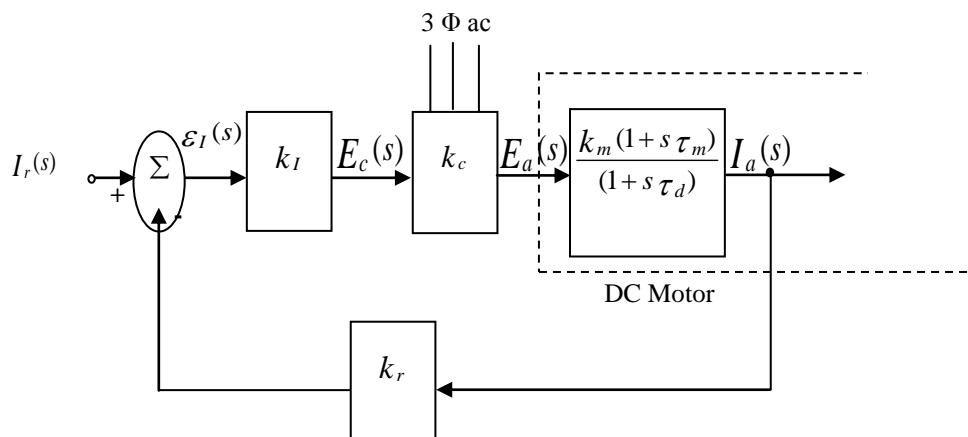


Fig. 4: Current-control loop

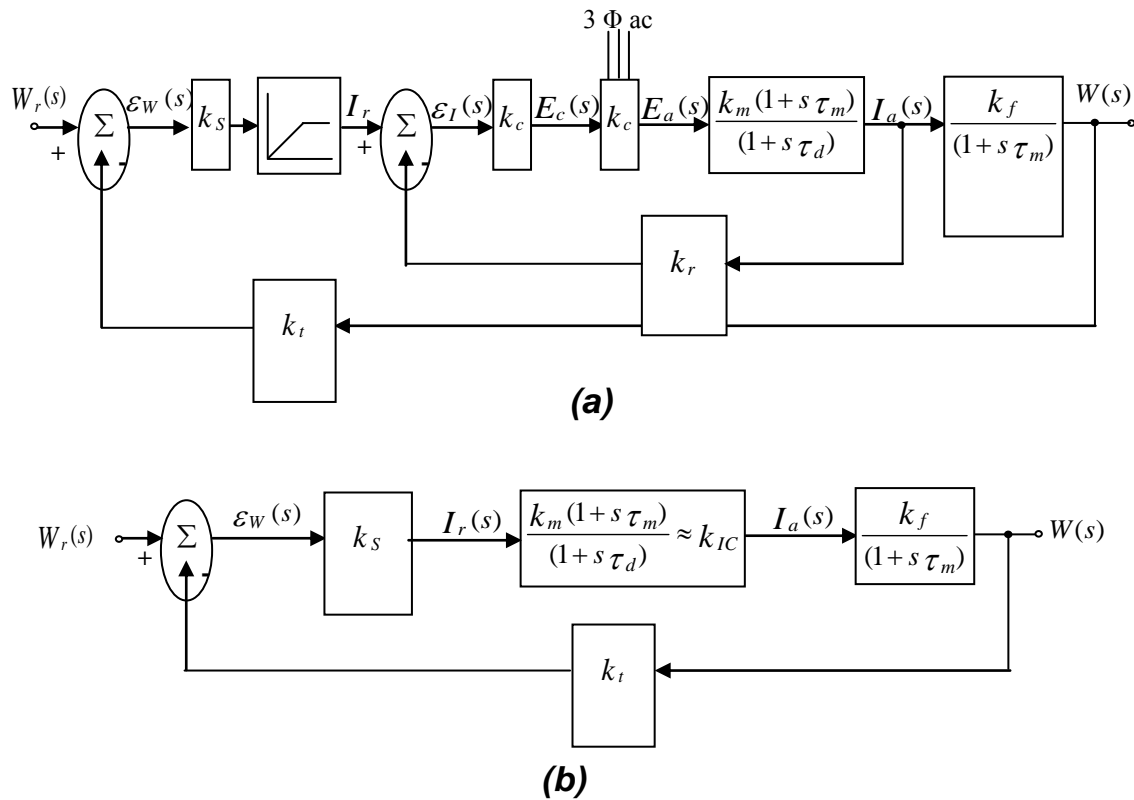


Fig. 5: Proportional speed control with inner current-control loop. (a) Functional block diagram. (b) Simplified functional block diagram

3. Design of Speed and Current Controllers

3.1. Proportional (P) Controller

The parameters and constants of a separately excited dc motor that used in the closed-loop speed control of dc drive are described in the Appendix. The clamping value of I_r is chosen to be 3A. The feedback gains k_r and k_t assumed are fixed at these values given in the Appendix. The proportional controller parameters k_s and k_I for speed and current controllers are chosen on the basis of steady-state error considerations, where

$$\varepsilon(\infty) = \frac{1}{1 + G(s)H(s)|_{s=0}}$$

For the current control loop

$$G(s)|_{s=0} = k_I k_c k_m, \text{ and } H(s)|_{s=0} = k_r$$

Thus

$$\varepsilon_I(\infty) = \frac{1}{1 + k_I k_c k_m k_r}$$

$$\therefore k_I = \frac{\frac{1}{10} - 1}{k_c k_m k_r \varepsilon_{I(\infty)}}$$

Where $\varepsilon_{I(\infty)}$ is the desired steady-state current error. A practical value might be 10%, then

$$k_I = \frac{10-1}{(2)(85.374)(0.00372)} = 14.169$$

In the same manner as k_I , the speed controller gain k_S can be calculated, In this case.

$$\varepsilon_W(\infty) = \frac{1}{1 + G(s)H(s)} \Big|_{s=0}$$

For the speed control loop

$$G(s) \Big|_{s=0} = k_S k_{IC} k_f \text{ and } H(s) \Big|_{s=0} = k_t$$

$$\therefore k_S = \frac{\frac{1}{0.25} - 1}{k_{IC} k_f k_t \varepsilon_N(\infty)}$$

Where $\varepsilon_N(\infty)$ is the desired steady-state speed error. For 0.25% error, $k_S = 19.407$. The system response is getting by using MATLAB package. Fig. 6 shows the current and speed responses of the system when the current and speed controller are proportional type controller, with reference speed 120rad/s.

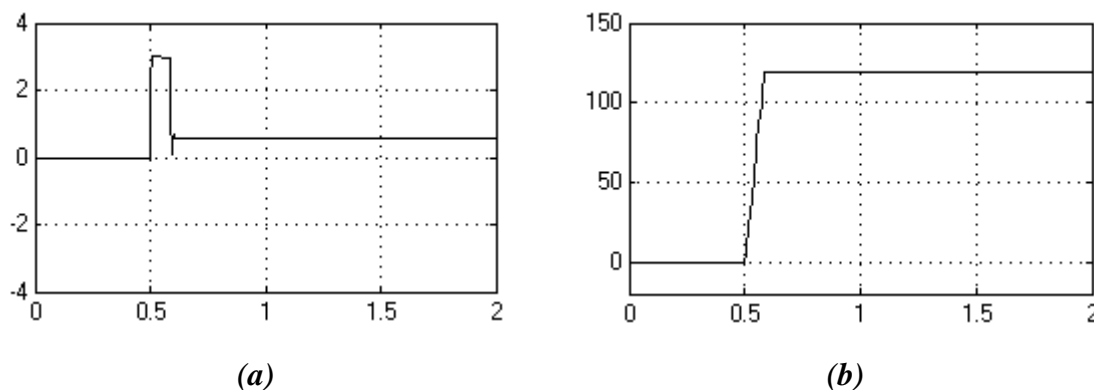


**Fig. 6: Response of proportional control to step change in speed reference
(a) Current response (b) Speed response**

3.2. Proportional-Integral (PI) Controller

To eliminate the steady-state error and to reduce the forward gain required, the proportional speed controller is replaced by a PI-type controller. The proportional plus integral type of controller has been used to achieve good dynamic and steady-state response [8]. The new controller transfer function is $k_S(1+s\tau_s)/s\tau_s$. The resulting block diagram is shown in Fig. 7.

The controller gain k_s and its pole $(1/\tau_s)$ can be designed from the consideration of damping and natural frequency. The overall transfer function becomes

$$\frac{W(s)}{W_r(s)} = \frac{k_s k_{IC} k_f \frac{(1+s\tau_s)}{(s\tau_s)(1+s\tau_m)}}{1 + \frac{k_s k_{IC} k_f k_t (1+s\tau_s)}{(s\tau_s)(1+s\tau_m)}} \tag{24}$$

$$= \frac{\frac{1}{k_t} (1+s\tau_s)}{1 + \tau_s \left(1 + \frac{1}{k_s k_{IC} k_f k_t}\right) s + \frac{\tau_s \tau_m}{k_s k_{IC} k_f k_t} s^2}$$

For $k_s k_{IC} k_f k_t \gg 1$

$$\frac{W(s)}{W_r(s)} = \frac{(1+s\tau_s)}{k_t \left(1 + s\tau_s + s^2 \tau_s \tau_2\right)} \tag{25}$$

Where

$$\tau_2 = \frac{\tau_m}{k_s k_{IC} k_f k_t} \tag{25a}$$

The characteristic equation of the system is

$$s^2 + \frac{1}{\tau_2} s + \frac{1}{\tau_s \tau_2} = 0$$

Then

$$2\zeta \omega_n = \frac{1}{\tau_2} \text{ or } \tau_2 = \frac{1}{2\zeta \omega_n}, \text{ also } \omega_n^2 = \frac{1}{\tau_s \tau_2}$$

Then $\tau_s = 2\tau_2$

For damping ratio of 0.707 and natural frequency is 10rad/s, both the gain k_s and the time constant τ_s can be calculated.

$$\tau_2 = 0.0707, \tau_s = 0.1414 \text{ and}$$

$$k_s = \frac{\tau_m}{k_{IC} k_f k_t \tau_2} = 1.720$$

Then the PI-controller transfer function is $(1.720 + (12.160)/s)$

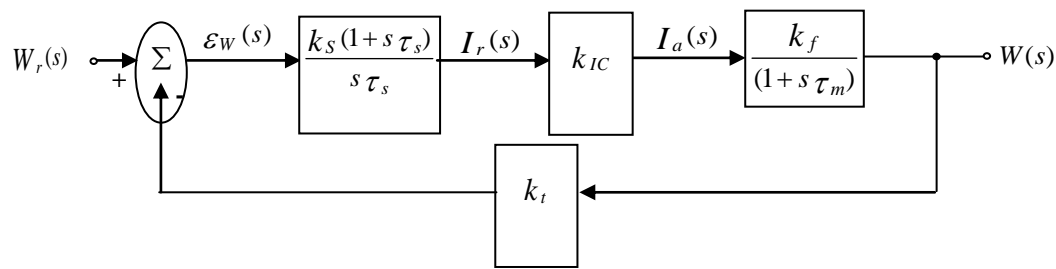


Fig. 7: Speed-control loop with PI-controller.

The simulation response for a PI-controller step change in speed reference is shown in Fig. 8.

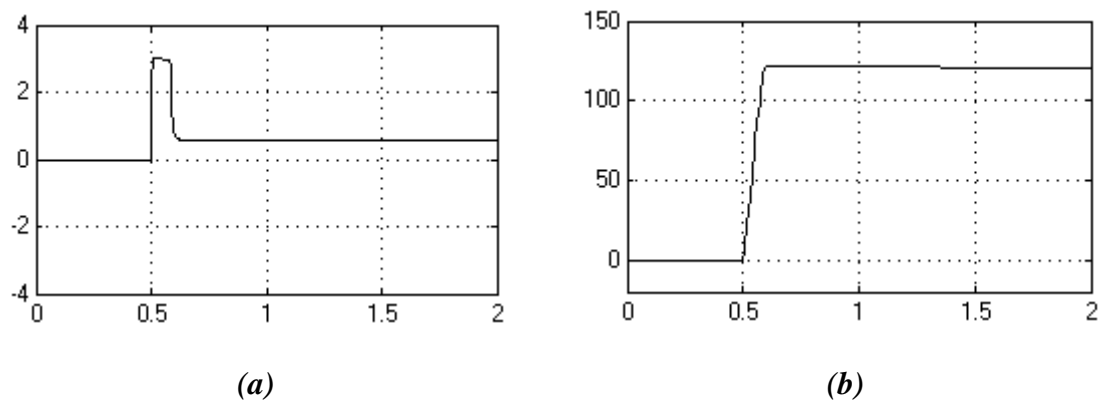


Fig. 8: Response of PI-control to step change in speed reference (a) Current response (b) Speed response

4. Soft-Starting Concept

According to equation 3, at starting, the back EMF is equal to zero because the speed is zero. Since the armature circuit resistance is small, then the armature starting current is very large and may be damage the converter switching device.

To reduce the dangerous of starting current a soft-starting concept is used. In this concept the armature voltage is increased in small steps over a short period at starting to ensure that the starting current in allowable values.

Fig. 9 and Fig. 10 are shows the system response with soft-starting technique by using proportional and proportional-integral controllers respectively.

It's clear from the current response that the starting current with this technique is less than without using soft-starting technique, but the transient speed response is slow down.

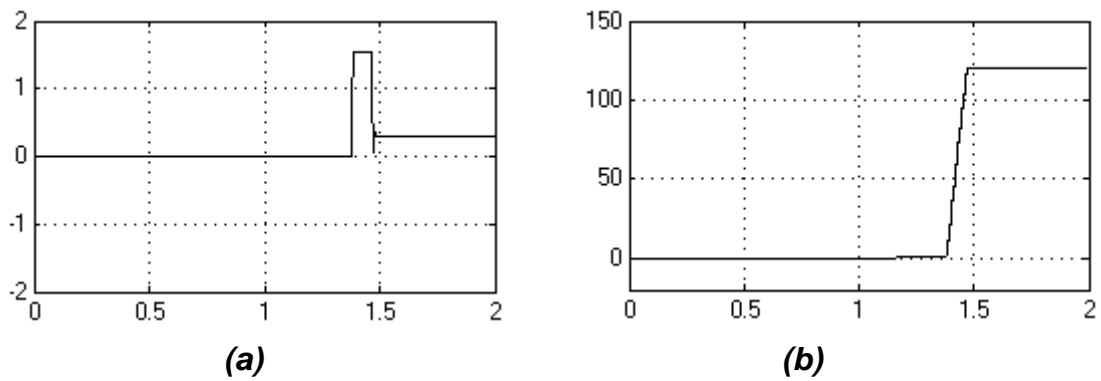


Fig. 9: Response of P-control to step change in speed reference with soft-starting technique (a) Current response (b) Speed response

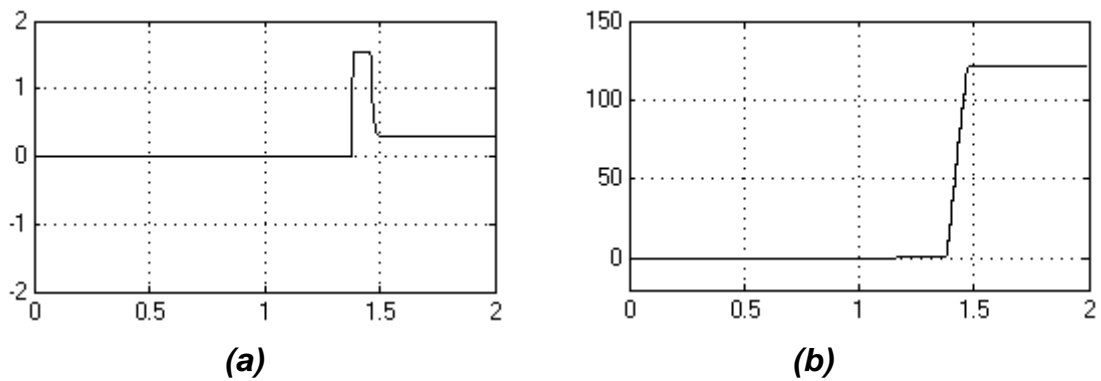


Fig. 10: Response of PI-control to step change in speed reference with soft-starting technique (a) Current response (b) Speed response

5. Step Increasing and Decreasing of Reference Speed

If the motor reference speed increase, the speed error ϵ_w increases. This in turn changes the firing angle of the converter, and thus increases the motor armature voltage E_a . An increase in the motor voltage develops more torque to increase the motor speed to reach approximately to the reference speed. Fig. 11 shows the speed and current responses for step increasing in the reference speed, while Fig. 12 shows the system response for decreasing reference speed case.

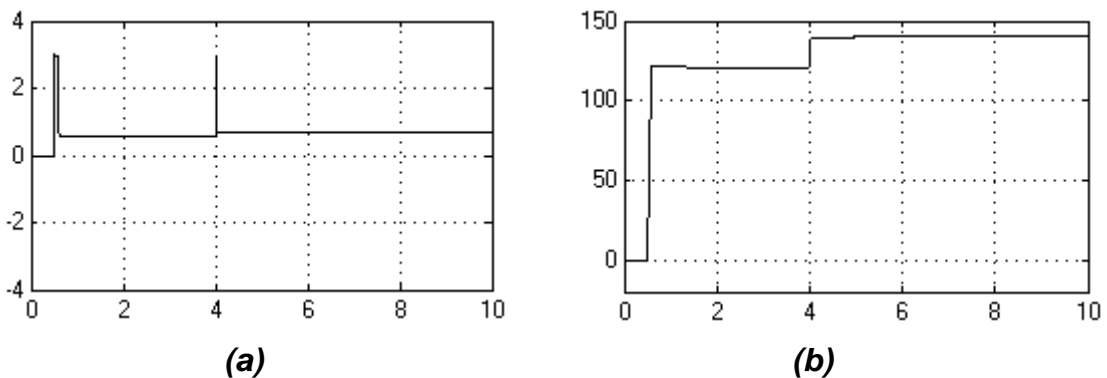


Fig. 11: Response of PI-control to step increasing in speed reference (a) Current response (b) Speed response

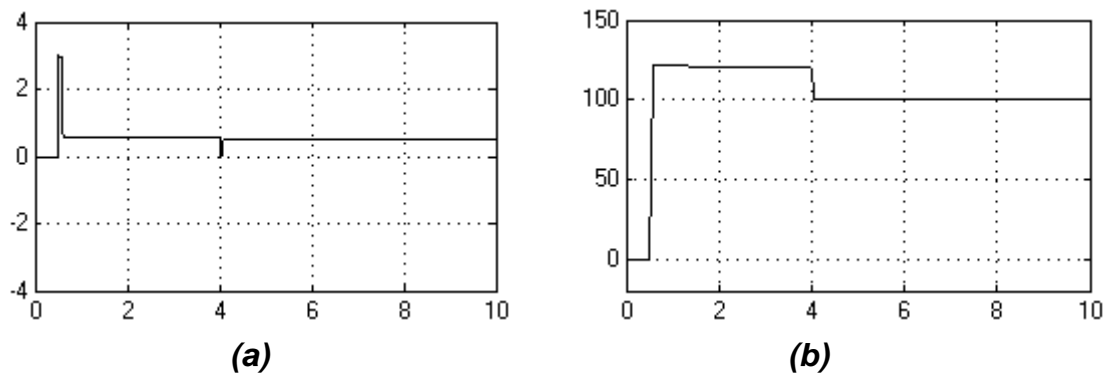


Fig. 12: Response of PI-control to step decreasing in speed reference (a) Current response (b) Speed response

6. Load Torque Disturbance

In some applications a load is suddenly applied to the motor, therefore the effect of such load torque disturbances is considered now in two cases.

6.1 Proportional (P)-Controller

Fig. 13a shows the complete block diagram for the speed loop with proportional speed controller. If changes in the reference speed W_r are neglected, an expression for the current can be written in terms of the speed change $W(s)$. From Fig. 13a

$$I_a(s) = \frac{1}{R} \{-k_a \phi \cdot W(s) + k_I k_c [-k_r I_a(s) + k_s (\frac{-k_t W(s)}{1+s \tau_t})]\} \tag{26}$$

$$I_a(s) = -[\frac{k_a \phi + \frac{k_I k_s k_c k_t}{1+s \tau_t}}{R_a + k_I k_c k_r}] W(s) \tag{27}$$

Since $k_I k_c k_s k_t \gg k_a \phi$ and $k_I k_c k_r \gg R_a$

$$I_a(s) \approx -\frac{k_s k_t}{k_r (1+s \tau_t)} W(s) \tag{28}$$

The block diagram then simplifies to that shown in Fig. 13b. Thus

$$\begin{aligned} \frac{W(s)}{T_L(s)} &= \frac{-\frac{1}{B+sJ}}{1 + (\frac{k_a \phi k_s k_t}{k_r (1+s \tau_t)}) (\frac{1}{B+sJ})} \\ &= \frac{-\frac{1}{B} (1+s \tau_t)}{k^1 [1 + s \frac{(\tau_m + \tau_t)}{k^1} + s^2 \frac{\tau_m \tau_t}{k^1}]} \end{aligned} \tag{29}$$

Where $k^1 = 1 + \frac{k_a \phi k_s k_t}{k_r B}$

Since $k_f = k_a \phi / B$ and $k_r \approx 1/k_{IC}$, then $k^1 = 1 + k_{IC} k_f k_s k_t$

Since $k_{IC} k_f k_s k_t \gg 1$

$$\frac{N(s)}{T_L(s)} \approx \frac{-1}{k_r} \frac{(1 + s \tau_t)}{1 + s(\frac{\tau_m + \tau_t}{k^1}) + s^2(\frac{\tau_m \tau_t}{k^1})} \tag{30}$$

The current response from equations (28) and (30) is

$$\begin{aligned} \frac{I_a(s)}{T_L(s)} &= \frac{I_a(s)}{W(s)} \cdot \frac{W(s)}{T_L(s)} \\ &= \frac{1}{k_a \phi \left(1 + s(\frac{\tau_m + \tau_t}{k^1}) + s^2(\frac{\tau_m \tau_t}{k^1}) \right)} \end{aligned} \tag{31}$$

This also shows a similar second-order response.

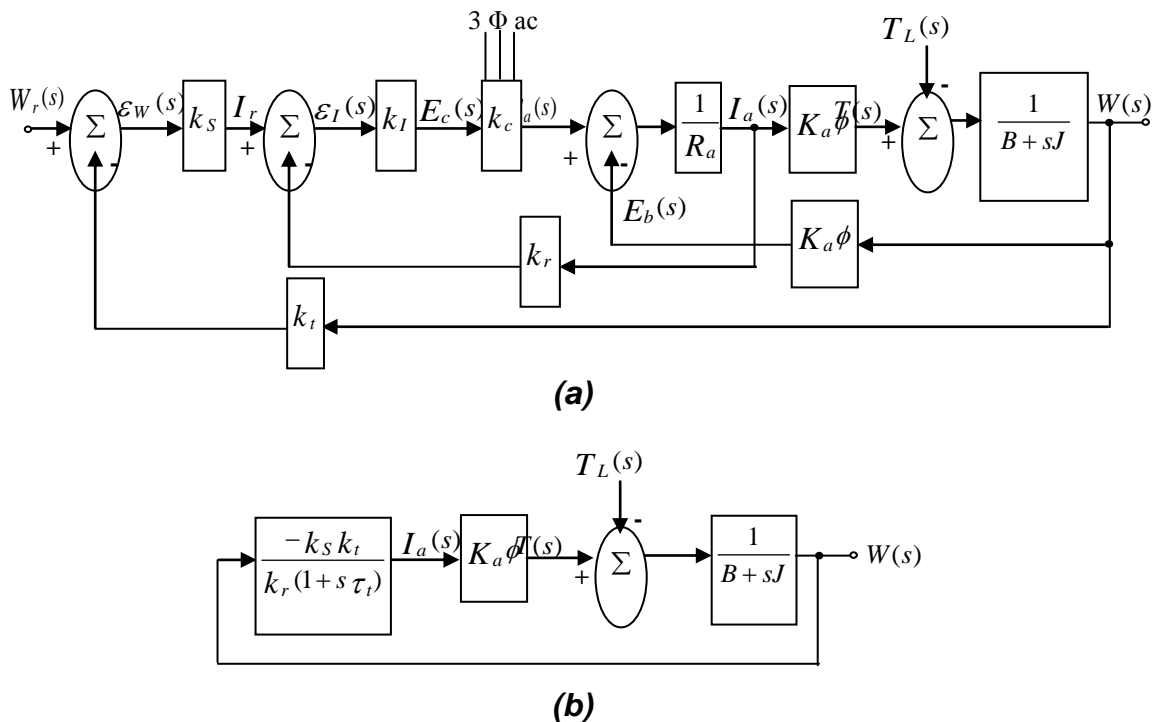


Fig. 13: Effect of load torque disturbances.

(a) Functional block diagram. (b) Simplified Functional block diagram.

Fig. 14 is the system response with proportional control to a step change in load torque. It can be seen that the response is second-order and that there is steady-state change in speed and current.

6.2. Proportional-Integral (PI)-Controller

The controller transfer function designated by k_s in Fig. 13a is replaced by the PI-transfer function $k_s(1 + s \tau_s) / s \tau_s$.

$$\frac{W(s)}{T_L(s)} = \frac{-\frac{1}{B+sJ}}{1 + \left(\frac{k_a \phi k_S k_t}{k_r}\right) \left(\frac{1+s\tau_s}{s\tau_s}\right) \left(\frac{1}{B+sJ}\right)}$$

$$= \frac{-\tau_s k_r}{k_a \phi k_S k_t} \frac{s}{1 + s\tau_s \left(1 + \frac{B k_r}{k_a \phi k_S k_t}\right) + s^2 \frac{\tau_s \tau_m B k_r}{k_a \phi k_S k_t}} \tag{32}$$

Because $\frac{k_a \phi k_S k_t}{B k_r} \gg 1$ then

$$\frac{W(s)}{T_L(s)} \approx \frac{-\tau_s k_r}{k_a \phi k_S k_t} \frac{s}{1 + s\tau_s + s^2 \tau_s \tau_2} \tag{33}$$

Where $\tau_2 = \frac{\tau_m B k_r}{k_a \phi k_S k_t}$

From Fig. 13b, for the PI-controller,

$$\frac{I_a(s)}{W(s)} = \frac{-k_S k_t (1 + s\tau_s)}{s\tau_s k_r} \tag{34}$$

Now, from equations (33) and (34),

$$\frac{I_a(s)}{T_L(s)} = \frac{I_a(s)}{W(s)} \cdot \frac{W(s)}{T_L(s)} \tag{35}$$

$$= \frac{1}{k_a \phi} \frac{(1 + s\tau_s)}{(1 + s\tau_s + s^2 \tau_s \tau_2)} \tag{36}$$

Fig. 15 shows the system response with PI-controller due to a step change in load torque. The transfer function in equation (33) has a zero at the origin. Therefore, there will be a no steady-state speed change for a step-change in load torque; this is shown in the Fig. 15b.

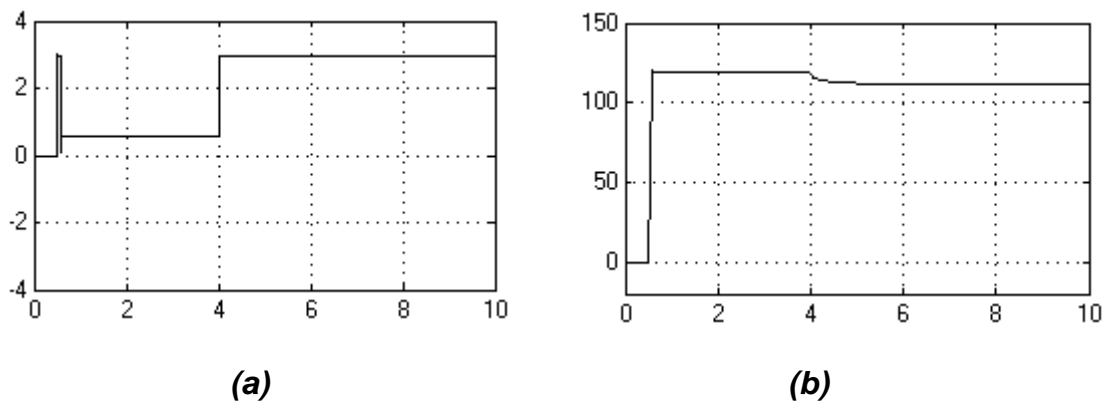


Fig. 14: Response to step increase in load torque with P-control (a) Current response (b) Speed response

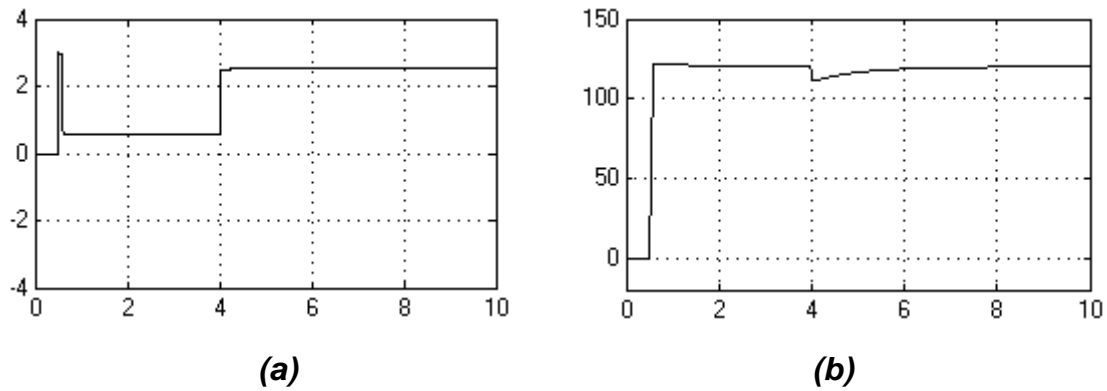


Fig. 15: Response to step increase in load torque with PI-control (a) Current response (b) Speed response

To reduce the dynamic speed variations of the dc motor due to the step change in load torque, a *feed forward* scheme is presented as shown in Fig. 16. In this scheme the required current I_L to compensate the disturbances effect of load torque is added to the reference current. The load current is computed as following. Since

$$W(s) = \frac{T(s) - T_L(s)}{B} \cdot \frac{1}{1 + s\tau_m} \tag{37}$$

Then

$$T_L(s) = T(s) - B(1 + s\tau_m)W(s) \tag{37a}$$

Since $I_L(s) = \frac{T_L(s)}{k_a\phi}$

$$\therefore I_L(s) = \frac{T(s) - B(1 + s\tau_m)W(s)}{k_a\phi} \tag{38}$$

Fig. 17 shows the response to step increase in load torque with PI-controller and feed forward loop.

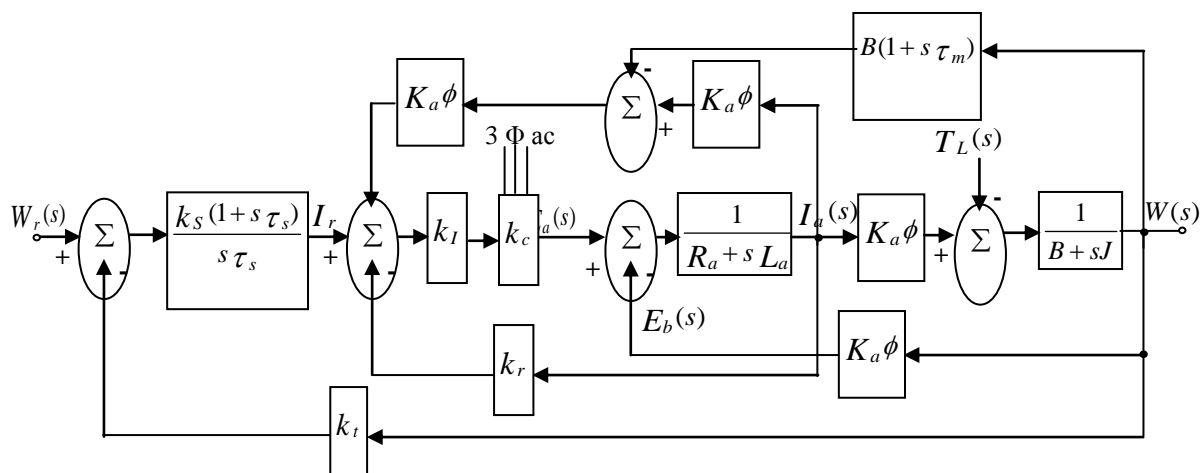


Fig. 16: Speed control of dc motor with feed forward loop

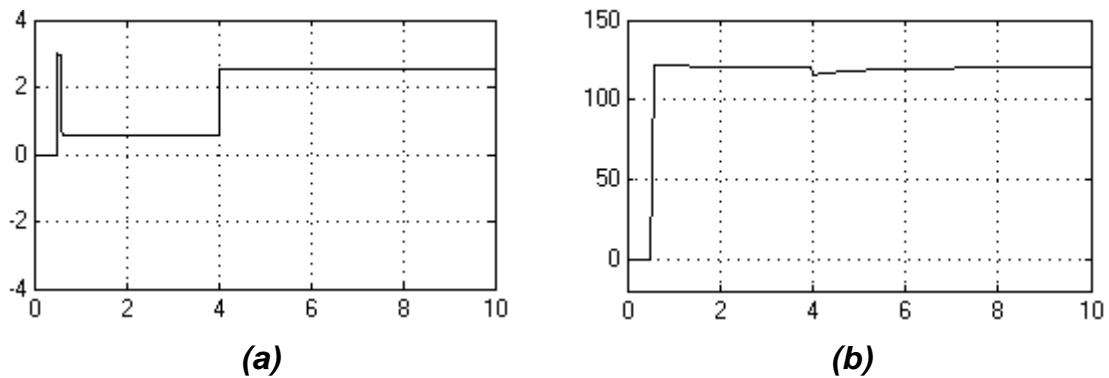


Fig. 17: Response to step increase in load torque with PI-control and feed forward control loop (a) Current response (b) Speed response

7. Conclusion

A closed-loop speed control of dc-motor system has been described. The closed-loop control technique is used instead of open-loop technique to increasing the accuracy, improved the dynamic response, and reduction of the effects of disturbances such as sudden loading. A transfer function technique is used to design the controller parameters. The current limiter is used to limit the armature current to some maximum allowable value (3A). The simulation response of the system is found for speed proportional-current proportional and speed proportional plus integral-current proportional controllers. The steady-state error is reduced by using PI-speed controller.

The overshoot of current greater than rated current is prevented by using soft-starting technique, but in this case the response of the system is slower than without soft-starting. The response of the system for step increasing and decreasing of reference speed is getting, and found that the output of the system $W(S)$ is tracked the reference speed $W_r(s)$. An improved response is achieved by using a feed forward loop with load torque case. The operation at a constant speed and control of speed over a wide range can be easily performed.

8. Appendix

The parameters and constants of a closed-loop control system for a separately excited dc motor drive are listed below:

8.1. DC Motor (180v, (1/3)hp, 3300rpm):

$R_a = 4\Omega$: Armature circuit resistance

$R_s = 0.5\Omega$: Sampling resistance

$L_a = 80mH$: Armature circuit resistance

$J=0.0025\text{Nms}^2/\text{rad}$: moment of inertia of motor and load

$B=0.001\text{ Nms}/\text{rad}$: Viscous friction of motor and load

$I_a=2.1\text{A}$: Rated current of motor

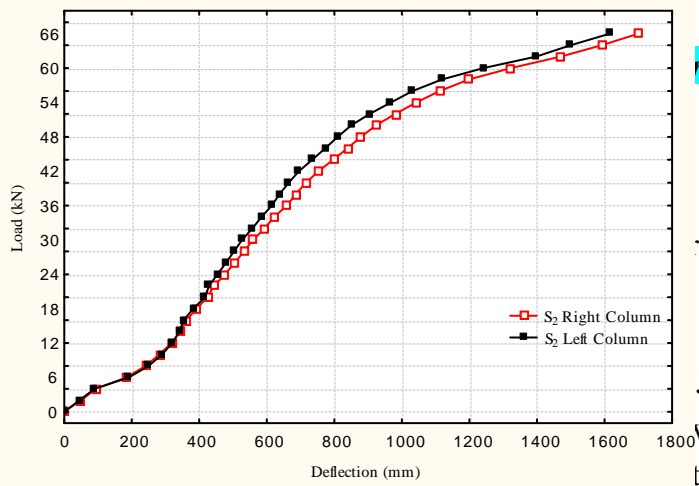
$k_a\phi=0.514\text{vs}/\text{rad}$: Back EMF and torque constant

8.2. Parameters and Constants

$\tau_a=20\text{ms}$, $\tau_m=2.5\text{s}$, $\tau_d=0.04187\text{s}$

$k_d=0.00372\text{A}/\text{v}$, $k_f=514\text{rad}/\text{s.A}$, $k_t=0.08\text{v.s}/\text{rad}$

$k_c=85.374$, $k_{IC}=2$, $k_r=(1/0.5)\text{v}/\text{A}$



C. Sen, “Analog and Digital Speed Control of DC Motor Using Proportional and Integral- Proportional Control Techniques” *Journal of Electronics*, Vol. IE-34, No. 2, May 1987, pp. 227-234.

John Wiley and Sons, 1981.

Sen, C. and A.K. Goel, “Firing Circuit for 3-Ø Variable Frequency Inverter”

4. B.R. Pelly, “Thyristor Phase - Controlled Converters and Cyclo Converters”, John Wiley and Sons, 1971.
5. Lander C.W. “Power Electronics”, McGraw-Hill, 1981.
6. Paresh C. Sen and Murray L. Macdonald, “Thyristorized DC Drives with Regenerative Braking and Speed Reversal” *IEEE, Transactions on Industrial Electronics and Control Instrumentation*, Vol. IECI-25, No. 4, Nov. 1978, pp. 347-354.
7. Ogata K. “Modern Control Engineering” Prentice-Hall, Englewood cliffs NJ, 2002.
8. T. Krishnan and B. Ramaswami, “Speed Control of DC Motor Using Thyristor Dual Converter” *IEEE, Transactions on Industrial Electronics and Control Instrumentation*, Vol. IECI-23, No. 4, Nov. 1976, pp. 391-399.